

Experimental and Thermal Analysis of Washing the Packed Ice Bed in Wash Columns

Frank G. F. Qin, Min Lin Yang, and Xiao Xi Yang

Research Center of Distributed Energy Resource System, DongGuan University of Technology, DongGuan City, China

Xiao Dong Chen

Dept. of Chemical Engineering, Monash University, Clayton Campus, VIC, Australia

Arjan Abeynaïke

Dept. of Chemical Engineering and Biotechnology, University of Cambridge, Cambridge CB2 3RA, U.K.

DOI 10.1002/aic.11912

Published online August 11, 2009 in Wiley InterScience (www.interscience.wiley.com).

In the process of freeze concentration (FC), the main problems in operating the counter-current wash column used for separating ice from ice slurries are channeling and viscous fingering. These phenomena lead to the mixing of pure water and mother liquid, as well as entrainment of mother liquid within the removed ice. Experimental and thermal analysis of the wash front interface in this research relates ice melting and wash front breakthrough with the operating conditions (such as the wash water temperature, ice bed temperature and porosity). Criteria for wash front stability are proposed. © 2009 American Institute of Chemical Engineers *AIChE J.* 55: 2835–2847, 2009

Keywords: freeze concentration, wash column, wash front and stability, channeling, viscous fingering, thermal analysis

Introduction

Many methods have been developed in chemical engineering for separating solid particulates from liquids, such as centrifugation, press filtration, vacuum filtration, and membrane filtration.^{1,2} Other methods include deposition and flocculation, etc. However, these methods proved not suitable for removing ice from ice slurries, not only because the ice particles in freeze concentration (FC) are very small—from $<10\ \mu\text{m}$ before ripening to about $100\text{--}200\ \mu\text{m}$ after ripening for $3\text{--}5\ \text{h}^3$ —but also because the ice particles melt and re-freeze in pressure driven filtration. This limits the pressure applied.

As an essential step of FC, the separation of ice from ice slurries determines the loss of solute in the process. Centrifugation has been widely used in chemical engineering to sep-

arate particles from liquids, e.g., to separate crystals from magmas. It has reportedly been used for separating ice from ice slurries.^{4–6} Nevertheless, our studies showed that the high strength of centrifugal force imposed on the ice cakes would cause the non-Darcy effect: the filtrate flux is not proportional to the pressure drop across the filter mesh. This may be due to the press-and-melt nature of ice: a portion of ice melts under the pressure and passes through the filter as liquid, then freezes again to form fine ice particles. Moreover, an ice crust can be formed against the filter via thawing and freezing under the centrifugal force. This blocks the channels in the interstices between the ice particles, increasing the power consumption required to overcome the resistance. Therefore, to separate ice from the ice slurries found in FC, centrifugation does not appear to be a good choice.

Among various separation methods, the wash column has its unique advantages in segregating ice from the ice slurry because the liquid does not need to overcome the surface tension in passing through the porous matrix of the ice bed. The ice slurry is a mixture of ice crystals and unfrozen

Correspondence concerning this article should be addressed to F. G. F. Qin at f.qin@auckland.ac.nz or X. D. Chen at dong.chen@eng.monash.edu.au

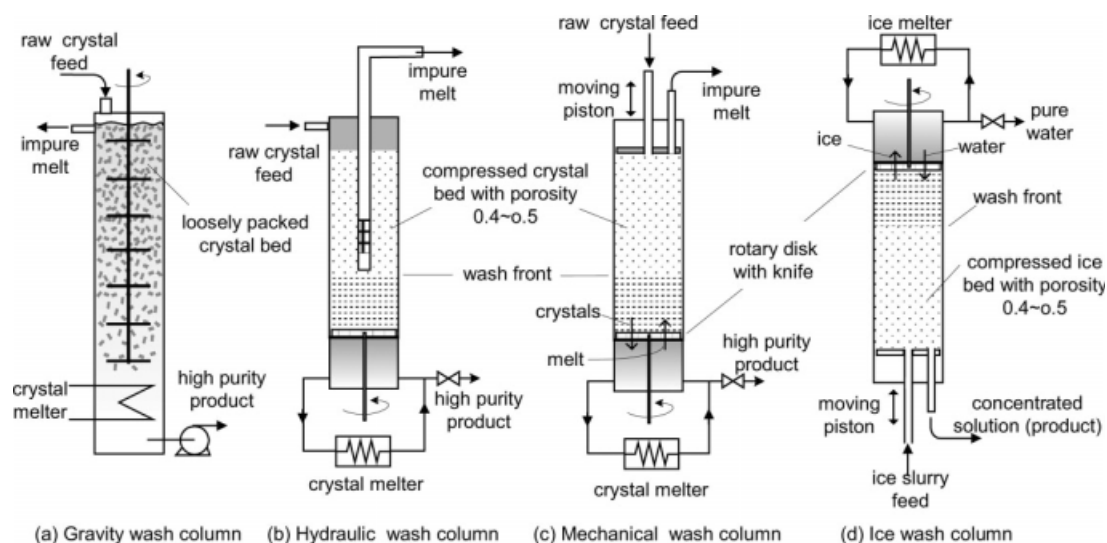


Figure 1. The schematic diagram of different wash columns used in industrial crystallization. (a) Gravity wash column, (b) hydraulic wash column, (c) mechanical wash column, and (d) ice wash column.

mother liquid. It is also a crystal magma usually produced from a subcooled scraped surface heat exchanger (SSHE). It is then fed into a suspension crystallizer, where small ice crystals ($0.1\text{--}10\text{ }\mu\text{m}$) gradually become larger by Ostwald ripening, an adiabatic process during which those very fine crystals, smaller than the thermodynamic critical size, melt; but the surviving crystals grow bigger.⁷ The permeability of the packed ice bed produced with the ice slurry also increases due to larger particle size.⁸

In a wash column, the ice slurry is compressed to form an ice bed, which is saturated with mother liquid. Wash water is introduced into the wash column on top and passes through the ice bed slowly to displace the mother liquid as a downward plug flow. The mother liquid usually has a greater specific gravity than the wash water, so that a horizontal wash front, a transitional region, can be seen between the upper washed ice and the lower unwashed ice. The washed ice is pushed up in the counter direction of the movement of the mother liquid and removed (together with the interstitial wash water) on top the wash column. Meanwhile, the concentrated mother liquid is withdrawn at the bottom (Figure 1d).

Counter-current wash columns have been used in some melt crystallizations, especially for viscous organic compounds, to separate crystals from melts.^{9–13} There are several kinds of wash column that cater for different applications. They are defined by their method of operation, e.g., gravity wash columns, hydraulic wash columns, and mechanical wash columns (Figure 1). Nevertheless, compared with many other solid–liquid separation methods, the technology of wash columns is often considered to be under development. Only a few relevant studies and applications have been reported. The wash column used for separating and purifying ice from ice slurries has different characteristics compared with those used in other melt crystallizations. For instance, ice is lighter in weight than the mother liquids and always tends to float; the washed (pure) ice is not melted inside the wash column normally (for producing washing water); and

there is only a very little amount of ice crystallization/re-crystallization taking place during the wash operation. This is quite different from the gravity wash column, which has been used for separating organic compound crystals from the melt. In a gravity wash column, crystals are purified by leaching and sweating, which actually involves continuous melting and re-crystallization in the journey of passing through the column.^{12,14}

Experimental

Apparatus and method

The experimental wash column is shown in Figure 2. It was made of a perspex cylinder with an inside diameter of 80 mm and height of 500 mm. The exterior was wrapped with 30 mm of rubber foam for thermal insulation, on which a double-glazed 30 mm \times 200 mm observation window was constructed at the upper section of the column.

The ice slurries were produced from a laboratory SSHE.^{15,16} The morphology of the ice was examined by a biological microscope placed in a cold cabinet.^{17,18} After aging for a given time, the ice slurry was quickly poured into the wash column for experimental study. The compressing force was provided by weight(s) on top of the mesh piston giving $0.1\text{--}0.4\text{ kg cm}^{-2}$ pressures. In this study, the pressure used was 0.1 kg cm^{-2} unless stated otherwise.

An ice-free section of mother liquid above the mesh piston was produced after compression. This part of the mother liquid was then drained to allow the liquid level to be flush with the ice bed surface. The mesh piston was kept in the wash column to maintain the pressure and prevent water rushing into the ice bed. A given amount of cold wash water was added into the column from the top until it reached the level marked “water line” before washing started. A ruler was placed beside the observation window to measure the thickness of the washed ice. During washing the mother liquid was drained into a measuring cylinder. The washing (or draining) rate was measured using a stopwatch.

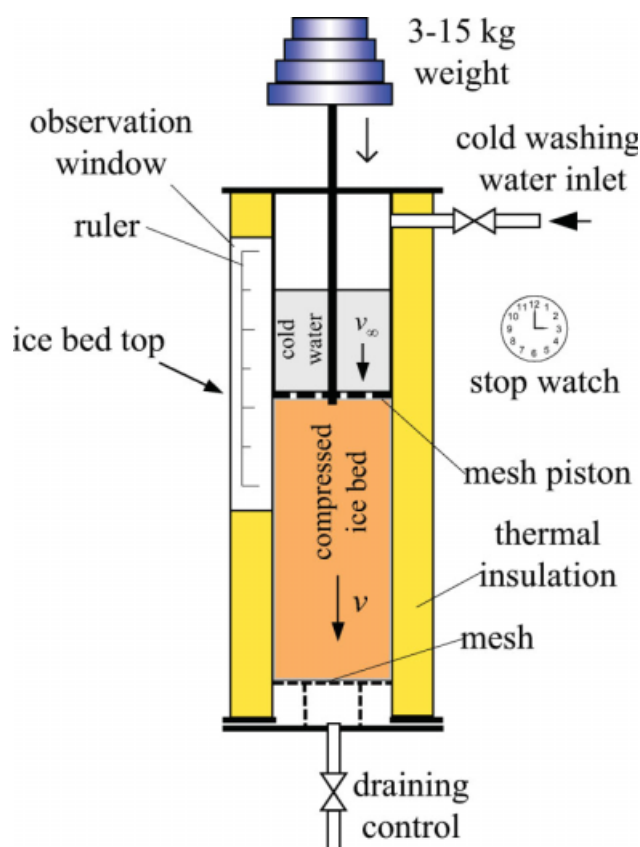


Figure 2. The experimental wash column.

[Color figure can be viewed in the online issue, which is available at www.interscience.wiley.com.]

The temperature distribution on the inside surface of the column was measured using six Type-T thermocouples of 0.5 mm diameter. The radial temperature distribution at the cross section at the wash interface was measured by four Type-T thermocouples of 0.5 mm diameter.

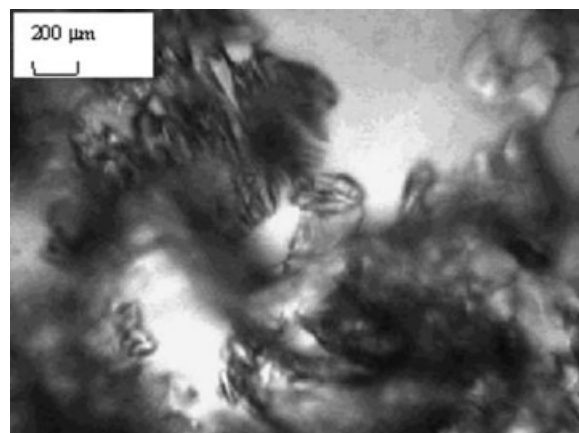
Experimental Results and Discussion

Morphology of the ice particles

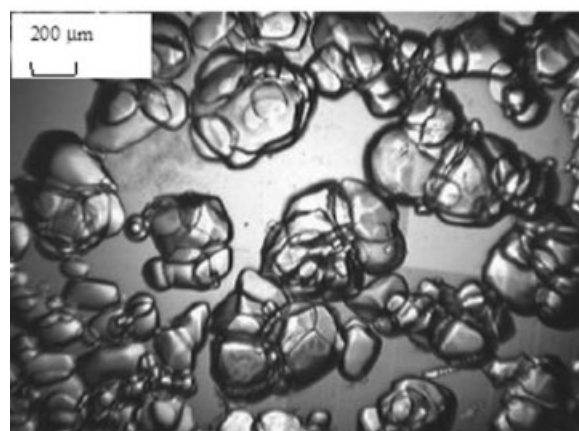
The newly formed ice particles are very small with irregular shapes as shown in Figure 3a. Most of them are dendrite debris of ice scraped off from the cooling surface. The cloudy mass in the picture without a clear boundary may consist of numerous smaller ice particles, which cohere as agglomerates.

The grain size of ice increases gradually during ripening. Agglomeration and re-crystallization may occur simultaneously. This can be seen in Figure 3b. The morphological change of ice during ripening has been studied by many and Ostwald ripening is usually said to play an important role in this process.^{19–22} Ice particles are forced to touch with the adjacent particles when being compressed in the wash column. The ice is at a subzero temperature before washing because of the freezing point depression (FPD) of the solution. However, the temperature approaches zero at the wash front when the ice is in contact with the wash water. Mild ice crystallization joins the ice particles to form a sinter-like matrix of ice, as shown in Figure 3c. Table 1 and Figure 4 show the temperature change on the inside surface of the wash column across the wash front.

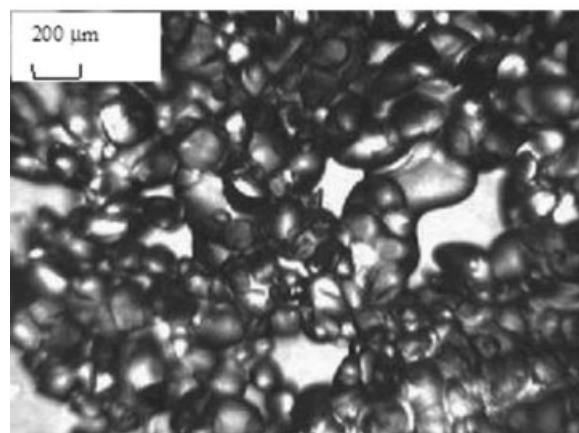
Table 2 and Figure 5 show the radial temperature profile at the cross section of the wash interface. It can be seen that the temperature at the interface is zero (or very close to



(a)



(b)



(c)

Figure 3. Micrograms of the morphological change of ice particles. (a) The ice dendrites scraped off from the cooling surface, (b) the ice particles during ripening, and (c) the porous, sinter-like structure of the washed ice bed (which was produced from the ice slurry ripened for 4 h).

Table 1. Temperature Distribution on the Inside Surface Along the Wash Column

Height (cm)	0	5	10	15	20	25
Temperature (°C)	−0.80	−0.63	−0.61	0.34	0.35	0.36

zero) except within about 0.5 mm of the sidewall. Note that the installation accuracy of the thin Type-T thermocouple restricted the measurable distance to the sidewall.

The experimental study showed that wash operation might fail due to a number of reasons, such as channeling, viscous fingering, and clogging, etc. These problems will be further studied in the following parts of this article.

Channeling and viscous fingering

Water and mother liquids are the so-called first-contact miscible liquids: when water displaces mother liquid in ice particle beds, mixing occurs. An often-seen undesirable problem is that a sharp, clear, horizontal wash front does not show up. Instead, the wash front is uneven or in the worst case no clear washed ice layer can be seen. The reason seems to be over mixing of the wash water with the mother liquid. However, careful observations (with the help of dye-tracer added in the mother liquid) showed that this might be attributed to two reasons: channeling and viscous fingering.

When local fractions of the ice bed progressively become loose during washing because of ice melting or migrating, channeling occurs. Channels appear as downward extending caves as shown in Figure 6. Viscous fingering occurs when the wash front moves faster at some places than others (see Figure 7). Unlike channeling, the local porosity in the vis-

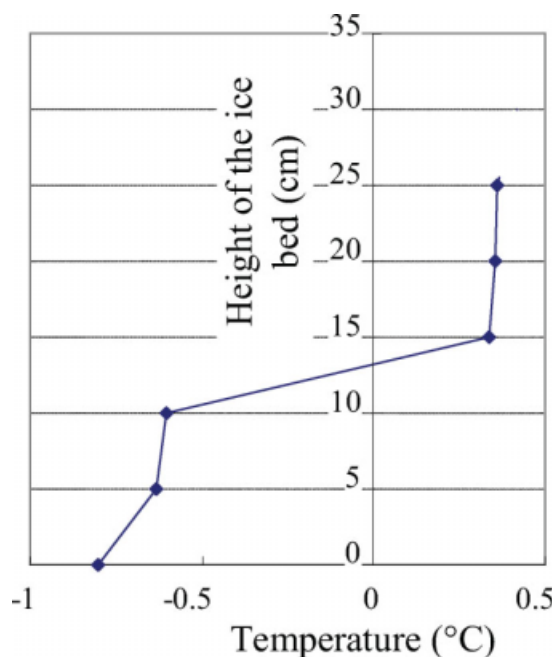


Figure 4. Temperature distribution on the inside surface along the wash column (wash water used was below 0.3°C).

[Color figure can be viewed in the online issue, which is available at www.interscience.wiley.com.]

Table 2. Temperature Profile Across the Wash Column at the Wash Interface

R (cm)	0	3.3	3.8	4	4.5	7.5
Temperature (°C)	0.37	0.39	0.39	0.63	2.8	18.70

R is the radial distance from the column center to the measured point.

cous fingering region does not appear to change. However, viscous fingering breaks through the horizontal displacing interface (wash front), so the separation of ice from the mother liquid becomes less efficient or even fails. Both channeling and viscous fingering often occur in the vicinity of the sidewall.

An uncompressed piled ice bed cannot be washed properly because particle cohesion and agglomeration cause the ice in the slurry to become lumpy. The interstices between ice lumps allow the liquid to run down faster than in other places. This causes channeling as illustrated in Figure 8a.

As mentioned before, both channeling and viscous fingering in a packed ice bed are related to ice melting or migration. Therefore, the temperature control of the wash water is critical. Figure 9 presents the effect of the wash water temperature on the wash performance of an ice bed. The bed temperature was measured to be -1.7°C , which was the freezing point of a 6% weight concentration of NaCl salt solution in the ice bed. The wash water temperature was reduced step by step from above 4°C to 0.1°C in a continuous counter-current wash column of a pilot scale FC system. The piston pressure in this run was set to 0.1 kg cm^{-2} . The experimental apparatus used for this run is not shown for intellectual property reasons. It can be seen that the experimental wash water temperature T_{we} must be kept below 1.5°C to achieve a desirable wash and separation result.

Freezing and clogging

If washing is done properly and a sharp wash front is formed, the ice bed can be slid out of the wash column after removing the supporting mesh at the bottom. The ice bed is rigid enough to stand by itself on the table as shown in Figure 10c. But unwashed ice beds (red part in the pictures) remain soft even though they were compressed.

A potential problem of water freezing is the clogging in the ice bed, which results from over-crystallization of ice in the porous ice bed. A high concentration of the mother liquid with its corresponding FPD will enhance this effect. A

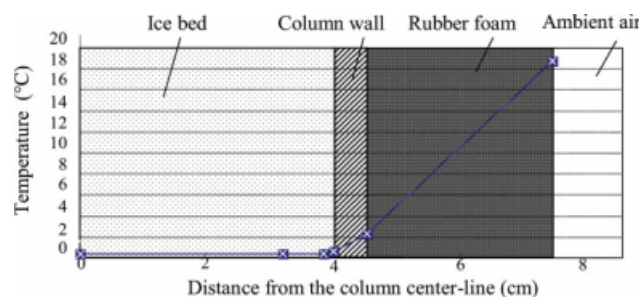


Figure 5. Radial temperature profile at the wash interface (the wash water used was below 0.5°C).

[Color figure can be viewed in the online issue, which is available at www.interscience.wiley.com.]

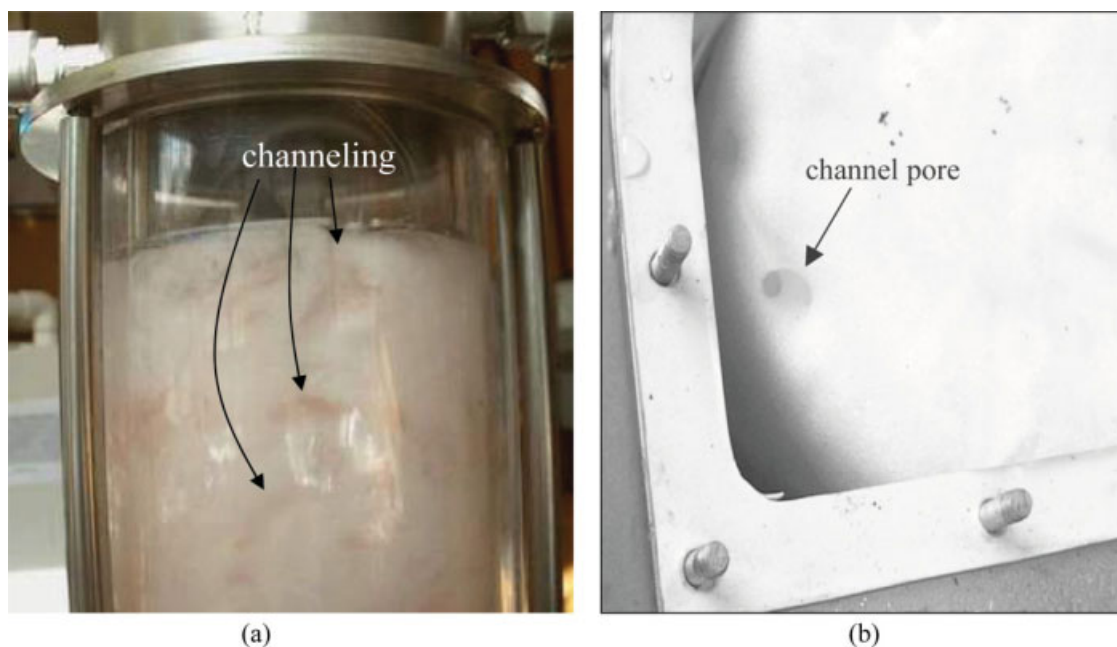


Figure 6. Channeling in the vicinity of the side wall. (a) A side view of channeling in the ice bed as downward caves and (b) a bird's eye view of channeling in the ice bed.

[Color figure can be viewed in the online issue, which is available at www.interscience.wiley.com.]

similar phenomenon was mentioned by others.^{23–25} Experiments in this study showed that it usually happened when the aging time of the ice was insufficient. Perhaps it was because the “premature” ice slurry contained a large amount of very fine ice particles so that the permeability was poor. The situation may become worse when the ice bed is over compressed for it will result in dead-end pores and occlusion of mother liquid inside ice lumps due to pressure-induced fusion of ice. Clogging of the ice bed increases the flow resistance and holds up the ice bed movement. The ice close to the wall may gradually melt and eventually lead to channeling. This is illustrated in Figure 8c.

Table 3 presents the experimental observations of the effect of the piston pressure on the wash performance. Zero pressure means that the ice bed was naturally piled up. As the applied pressure was increased from 0 to 5 kg, the wash gradually became better. When the pressure increased to 10 kg and higher, the movement of the wash interface gradually became sluggish. When the pressure was somewhat higher than 40 kg, partial clogging might form because the packed ice bed started to show unwashed parts, and then partial channeling started to appear at the vicinity of the wall.

Axial dispersion

The solution was dyed red to facilitate the observation in this work. Photographs in Figure 10 illustrate the influence of ripening time (and the grain size of the ice) on the axial dispersion in the wash column. The ice grains were initially very small, e.g., $<10\ \mu\text{m}$, with irregular shapes. They increased to $\sim 200\ \mu\text{m}$ in diameter after ripening for 3–6 h (Figure 3). Similar and indeed perhaps more details have already been reported by others previously.^{3,7,21,22,26} Experiments in this study show that washing cannot produce a

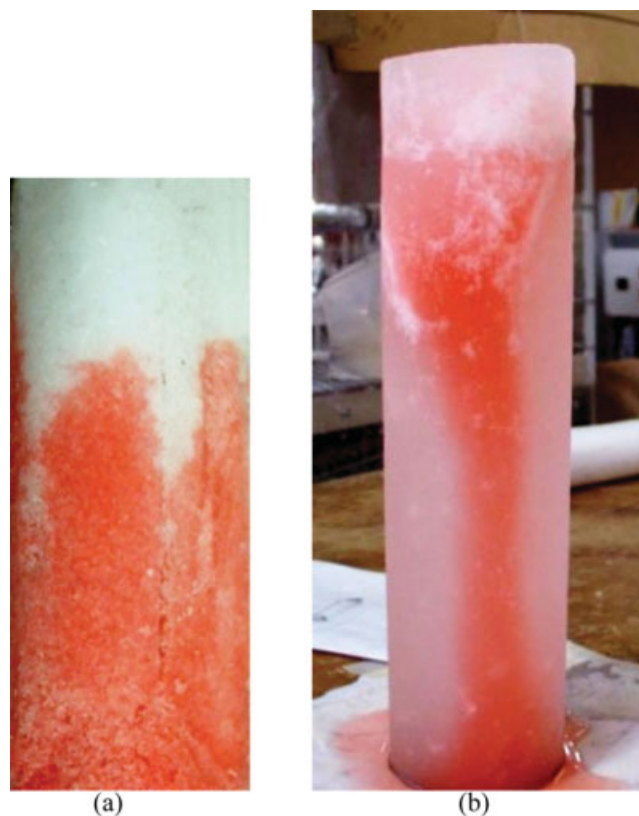


Figure 7. Viscous fingering at the wash front.

(a) Initial viscous fingering and (b) developed viscous fingering. [Color figure can be viewed in the online issue, which is available at www.interscience.wiley.com.]

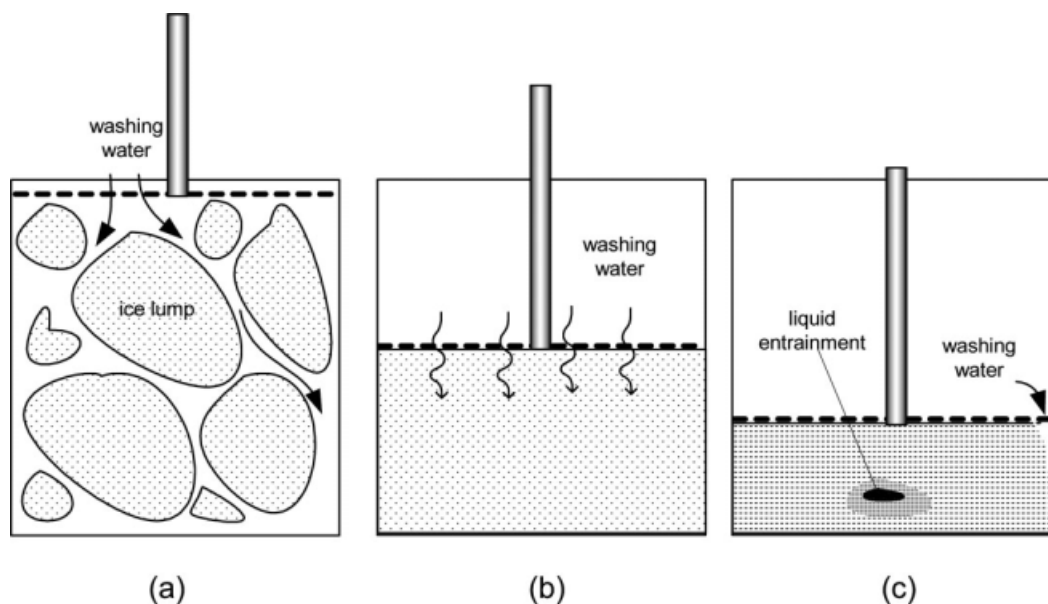


Figure 8. Schematic diagram of different behaviors in washing process.

(a) Loosely piled ice bed, (b) evenly and moderately compressed ice bed, and (c) over-compressed ice bed, this may possibly cause liquid entrainment and ice bed clogging, which ends up with ice melting at the outside bed.

sharp, horizontal wash front in the ice bed if it is produced from a premature ice slurry. This is shown in Figure 10a where the wash front is very fuzzy, implying that over mixing of the wash water and mother liquid must have taken place. In contrast, we are assured that the wash front will become sharper and clearer if the ice slurry is given a longer ripening time (Figure 10c).

In other words, the effective axial dispersion coefficient increases greatly as the ice grain size reduces. As the dimension of the pore canal should be in the same order of magnitude as the ice grains, this means that the larger the grain size in the ice bed, the smaller the effective axial dispersion coefficient. This cannot be well explained with the current dispersion theories of miscible fluids in porous media, which predicts an opposite trend.^{27–29} This is surprising, however, further discussion and analysis regarding the dispersion coefficient in porous ice beds is not the focus of this article.

Porosity and permeability

Ice grain size plays an important role in washing. First, it determines the porosity and permeability of the (compressed) ice bed. Second, it impacts the wash front range—the thickness of the transitional layer, which represents the degree of mixing between water and the concentrated solution. For the ice slurries produced by a SSHE, a larger grain size can only be obtained by providing appropriate ripening conditions and sufficient time. An ice bed compressed from a premature ice slurry shows poor permeability due to the small grain size.⁸ If the bulk permeability is too small, the wall effect will become significant because (1) the porosity at the outer boundary of the ice bed is greater and (2) the heat import from the environment tends to melt the ice in this region. The wall effect produces a weak region for the breakthrough of the wash front.

Theoretical Analysis

Mobility ratio

If there are two miscible liquids, when one liquid displaces another in a porous medium, an important criterion for a stable displacing front is that the mobility ratio $M < 1$.²⁷ M is defined as:

$$M = \frac{K_w/\eta_w}{K_l/\eta_l} \quad (1)$$

where K_w and K_l are permeabilities of the ice particle bed for water (in the washed layer) and mother liquid (in the unwashed layer), respectively. η_w and η_l are the viscosities of water and mother liquid, respectively.

If there is neither freezing nor thawing during the washing of the ice bed, its porosity will be the same before and after

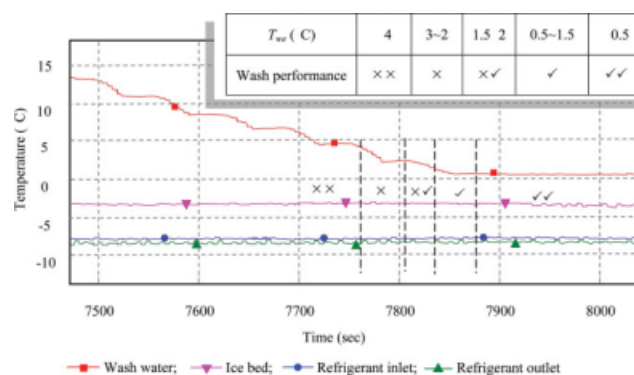


Figure 9. The effect of wash water temperature on the wash performance (the piston pressure is set to 0.1 kg cm^{-1} and the aging time of the ice slurry was about 3 h).

[Color figure can be viewed in the online issue, which is available at www.interscience.wiley.com.]

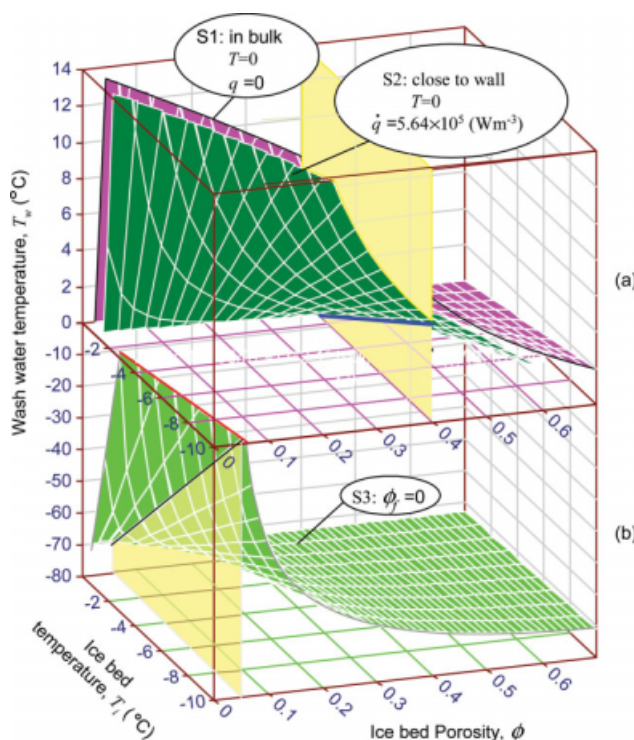


Figure 12. The operating conditions of the wash column. (a) Conditions that keep the contact temperature to be $T = 0^\circ\text{C}$. Surface S1 is for the inside of the ice bed, and S2 is for the region close to the wall and (b) conditions that cause clogging of the ice bed, which is on surface S3, where $\phi_f = 0$.

[Color figure can be viewed in the online issue, which is available at www.interscience.wiley.com.]

through in a unit time. ΔS is the cross-sectional area of the layer. ρ_i , c_i , and T_i are the density, thermal capacity, and temperature of ice, respectively. ρ_w and c_w are the density and thermal capacity of the wash water. T_w is the temperature of wash water just before it arrives to the wash front (not the temperature in the wash water reservoir). ϕ is the porosity of the ice bed. \dot{q} is the heat source function representing the heat released in a unit time and in a unit volume of the ice bed. An actual heat source can be internal (caused by chemical reactions for example) or external (caused by radiation or conduction, etc).

The left-hand side of Eq. 2 represents the heat taken up by the ice when the temperature increases from T_i to T . The right-hand side represents the heat being transferred to the ice, which includes the fraction released by the water (the first term) and the fraction released by the heat source (the second term). Equation 2 can be simplified by dividing both sides with the element volume ($\Delta z \Delta S$):

$$\rho_i c_i (1 - \phi) (T - T_i) = \rho_w c_w \phi (T_w - T) + \dot{q} \quad (3)$$

where

$$T = \frac{B_{wi} B_\phi T_w + T_i + \dot{q} / [\rho_i c_i (1 - \phi)]}{1 + B_{wi} B_\phi} = \frac{B_{wi} B_\phi T_w + T_i}{1 + B_{wi} B_\phi} + \frac{\dot{q}}{\rho_i c_i (1 - \phi) + \rho_w c_w \phi} \quad (4)$$

where $B_{wi} = \frac{\rho_w c_w}{\rho_i c_i} \approx \frac{1 \times 10^3 \times 4.2 \times 10^3}{0.917 \times 10^3 \times 2.1 \times 10^3} \approx 2.18$ and $B_\phi = \frac{\phi}{1 - \phi}$.

There are three possible values of the first contact temperature (T):

If $T > 0^\circ\text{C}$, ice melts. Over thawing of ice may lead to wash front breakthrough and channeling;

If $T = 0^\circ\text{C}$, ice bed is stable; and

If $T < 0^\circ\text{C}$, ice grows, forming a sinter-like structure in the washed, porous ice bed.

With $T = 0$ in Eq. 3, which is the freezing point of pure water, one has:

$$T_w = -\frac{\rho_i c_i (1 - \phi)}{\rho_w c_w \phi} T_i - \frac{\frac{\rho_i c_i (1 - \phi)}{\rho_w c_w \phi} + 1}{\rho_i c_i (1 - \phi) + \rho_w c_w \phi} \dot{q} = -\frac{T_i}{B_{wi} B_\phi} - \frac{\frac{1}{B_{wi} B_\phi} + 1}{\rho_i c_i (1 - \phi) + \rho_w c_w \phi} \dot{q} \quad (5)$$

where T_w is a specific wash water temperature at which the ice at the wash front will neither grow nor melt, i.e., the sensible heat exchanged in the first contact between water and ice (in the region of $\Delta z \Delta S$) does not result in phase change. The heat source function \dot{q} does not exist inside the bulk ice bed (assuming that no chemical reaction and no electromagnetic radiation are involved; this is a safe assumption in this case), but it may become significant in the vicinity of the sidewall. \dot{q} is positive when the ambient temperature is above the freezing point temperature of the mother liquid, indicating that thawing is more likely to happen on the outside of the ice bed rather than inside it, as shown in the region 3 of Figure 11. Therefore, thermal insulation of the wash column is definitely beneficial.

Although the first contact temperature (T) can be positive or negative, after the so-called "first contact" the actual temperature will always quickly approach zero because: (1) ice would melt if $T > 0^\circ\text{C}$ or grow if $T < 0^\circ\text{C}$, both leading to the equilibrium temperature of 0°C and (2) the interstices between ice particles in the ice bed would be smaller than the particle size, and in such a compact porous medium thermal equilibrium at the wash front would be achieved quickly.

One case that needs to be considered is when the porosity of the ice bed is uneven as illustrated in Figure 11. For example, if region 2 is looser than region 1, i.e., $\phi_2 > \phi_1$, the local interstitial flow velocity in region 2 would be greater than that in region 1, i.e., $v_2 > v_1$. This would result in the water temperature in region 2 being higher than that in region 1, $T_{w2} > T_{w1}$. Now, if T_2 happens to be above zero, ice in region 2 would thaw, resulting in ϕ_2 increasing further, which in turn increases the local flow velocity and eventually leads to a breakthrough of the wash water in region 2. This is briefly expressed as:

$$\phi_2 > \phi_1 \Rightarrow v_2 > v_1 \Rightarrow T_{w2} > T_{w1} \Rightarrow T_2 > T_1 \xrightarrow{\text{if } T_{w2} > 0^\circ\text{C}} \phi_2 \uparrow \Rightarrow \text{channeling in region 2}$$

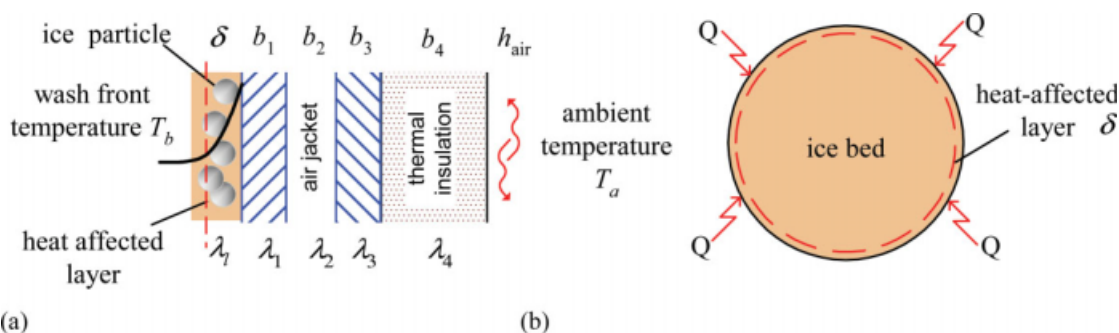


Figure 13. Double-glazed perspex wall plus rubber-foam for thermal insulation of the wash column. (a) Double-glazed wall with air jacket and (b) heat flux from environment to form a heat-affected layer.

[Color figure can be viewed in the online issue, which is available at www.interscience.wiley.com.]

That is to say, channeling is a result of a positive-feedback process.

The wall effect in a packed bed normally leads to a greater porosity close to the wall than that in the bulk.¹ The heat input from the environment is expected to increase this trend. Channeling is most likely to occur in this region, i.e., in region 3 of Figure 11. This has been confirmed by experimental observation as shown in Figure 6a.

In the bulk of the ice bed, where the heat source function can be ignored, i.e., $\dot{q} = 0$, Eq. 5 is simplified to the following:

$$T_w = -\frac{T_i}{B_{wi}B_\phi} = -\frac{\phi T_i}{(1-\phi)B_{wi}} \approx -\frac{\phi T_i}{2.18(1-\phi)} \quad (6)$$

The porosity (ϕ), the ice bed temperature (T_i), and the wash water temperature (T_w), construct a 3D space in Cartesian coordinate system. Equation 6 is represented by the surface S1 in Figure 12a, at which $T = 0^\circ\text{C}$. Above the surface, where $T > 0^\circ\text{C}$, ice melts at the wash front. Under the surface, where $T < 0^\circ\text{C}$, ice grows instead.

Criterion of wash front clogging

When the first contact temperature (T) is negative, i.e., $T < 0^\circ\text{C}$, the wash water may partially freeze, so that the porosity of the washed ice bed should decrease. Equation 4 predicts that, if the heat source is ignored ($\dot{q} = 0$), a lower porosity (ϕ) and a lower original ice bed temperature (T_i) will produce a lower value of T . The growing ice may join the separate ice particles to form a sinter-like ice cake in the washed ice bed, as we have seen in Figure 3c. Over-crystallization of ice would significantly reduce the bed porosity. The final porosity, ϕ_f , is determined by how much ice is produced. The energy balance of this process can be written as:

$$\rho_w c_w \Delta z \Delta S \phi T_w + \Delta H \rho_i \Delta z \Delta S (\phi - \phi_f) = -\rho_i c_i \Delta z \Delta S (1 - \phi) T_i \quad (7)$$

where $\rho_w c_w \Delta z \Delta S \phi T_w$ represents the sensible heat released by the interstitial water from its original temperature T_w to the freezing point (0°C) at the wash front. $\Delta H \rho_i \Delta z \Delta S (\phi - \phi_f)$ represents the latent heat released by the frozen water which causes the porosity change from ϕ to ϕ_f , and $-\rho_i c_i \Delta z \Delta S (1 - \phi) T$ represents the sensible heat taken up by

ice when the temperature changes from its original temperature (T_i) to the freezing point (0°C).

Re-arranging this equation, yields:

$$\phi_f = \phi + \frac{\rho_i c_i (1 - \phi) T_i + \rho_w c_w \phi T_w}{\Delta H \rho_i} \quad (8)$$

Letting $\phi_f = 0$ in Eq. 8 yields:

$$T_w = -\frac{\rho_i \phi \Delta H + \rho_i c_i (1 - \phi) T_i}{\rho_w c_w \phi} \quad (9)$$

This means that if the wash water temperature (T_w) were given by Eq. 9, the growth of ice would cause the porosity at the wash front to be zero. To illustrate the necessary condition, variables of ϕ , T_i , and T_w are used to construct a 3D space again. Equation 9 generates a surface S3 in Figure 12b, on which $\phi_f = 0$. Above S3, $\phi_f > 0$. Therefore conditions above S3 prevent the ice bed from clogging. Generally speaking, since the wash water is unlikely to reach the sub-freezing temperatures, ice bed clogging is unlikely to happen, unless the ice particle is very small (premature) and the ice bed is over compressed, as we have observed in experiments shown in Table 3. When the piston press increases to 30 kg or above, washing the ice bed becomes very difficult because of its poor permeability.

However, the ice bed may be unevenly compressed or packed to some extent. If a local original porosity value (ϕ) is close to zero, consequently its final porosity (ϕ_f) is likely to approach zero as well. Permeability in this part becomes worse and washing will be uneven. If ϕ_f approaches zero in the overall cross-sectional area of the wash front, the axial permeability of the ice bed will approach zero as well, because all interstices at the wash front are filled up by newly formed ice. Washing cannot proceed further.

Therefore, a feasible operating condition can be achieved by controlling the three parameters as follows: the original porosity of the ice bed (ϕ) at 0.25–0.5, the ice bed temperature (T_i) between -1 and -8°C (depending on the FPD of the mother liquid) and the wash water temperature (T_w) close to 0°C . Washing will be more likely to proceed in the region slightly above the horizontal plane, where $T_w = 0$ ($^\circ\text{C}$). Although it is unlikely that the entire ice bed will become clogged, there may be local regions where fusion

Table 4. Estimations of the Heat Transfer Coefficient (U) and the Heat Source Function (F_h)

Insulation scheme	U	\dot{q}	U	\dot{q}	U	\dot{q}	U	\dot{q}	U	\dot{q}
	$\delta = 0.1 \text{ mm}$		$\delta = 0.25 \text{ mm}$		$\delta = 0.5 \text{ mm}$		$\delta = 1 \text{ mm}$		$\delta = 2 \text{ mm}$	
Single shell	7.9	1580000	7.9	632000	7.9	316000	7.9	158000	7.9	79000
Double glazed	2.82	564000	2.82	225600	2.82	112800	2.82	56400	2.82	28200
Double glazed plus rubber foam	1	201680	1	80650	1	40300	1	20130	1	10050

U , $\text{Wm}^{-2} \text{ } ^\circ\text{C}^{-1}$, \dot{q} , Wm^{-3} .

The ambient temperature is assumed to be 20°C . The wall material is clear perspex.

and cohesion of ice result in liquid-sacs or dead-end pores inside the ice lumps. This situation is most likely to occur at the region close to the intersectional line of the surface (S3) and the horizontal plane ($T_w = 0^\circ\text{C}$), i.e., the red line in Figure 12b.

Heat source function

In Eq. 5, the heat source function (\dot{q}) is assumed to be zero inside the ice bed so that we have Eq. 6. At the boundary of the ice bed near the wall, however, we may need to consider the impact of the heat exchange with the environment, where \dot{q} cannot be ignored. The numerical value of \dot{q} is estimated later.

It is assumed that there is a heat-affected layer at the boundary of the outer ice bed close to the wall, in which the heat input from the environment is able to melt, more or less, the ice particles as illustrated in Figure 13. The overall heat transfer coefficient (U) on the double-glazed jacketed wall of the wash column can be expressed as:

$$\frac{1}{U} = \frac{\delta}{\lambda_l} + \frac{b_1}{\lambda_1} + \frac{b_2}{\lambda_2} + \frac{b_3}{\lambda_3} + \frac{b_4}{\lambda_4} + \frac{1}{h_{\text{air}}} \quad (10)$$

The heat transfer between the rubber foam surface and ambient air is by natural convection with a low individual heat transfer coefficient (h_{air}). An estimated value, $h_{\text{air}} = 10 \text{ Wm}^{-2} \text{ } ^\circ\text{C}^{-1}$, is used in this study.¹ Other values used in Eq. 10 are listed later:

The acrylic (perspex) jacket wall thickness is $b_1 = b_3 = 5 \times 10^{-3} \text{ m}$, the thermal conductivity $\lambda_1 = \lambda_3 = 0.188 \text{ Wm}^{-1} \text{ } ^\circ\text{C}^{-1}$. The air-layer thickness in the jacket is $b_2 = 5 \times 10^{-3} \text{ m}$, its thermal conductivity $\lambda_2 = 0.025 \text{ Wm}^{-1} \text{ } ^\circ\text{C}^{-1}$. The rubber foam thickness is $b_4 = 30 \times 10^{-3} \text{ m}$, and its thermal conductivity $\lambda_4 = 0.047 \text{ Wm}^{-1} \text{ } ^\circ\text{C}^{-1}$.

The thickness of the heat-affected layer (δ) is taken as a value that should fall into the range of a single ice particle size as a first approximation or several times of the single ice particle size. This means ice melting in this range would eliminate a whole grain of ice, greatly increasing the chance of channeling. Assuming the average diameter of an ice particle is $100 \text{ } \mu\text{m}$, we can simulate the value of δ varying from 100 to $2000 \text{ } \mu\text{m}$. The average thermal conductivity of the ice slurry can be estimated to be:

$$\lambda_l = 0.5\lambda_{\text{ice}} + 0.5\lambda_i \cong 0.53 \text{ Wm}^{-1} \text{ } ^\circ\text{C}^{-1}$$

Therefore, the overall heat transfer coefficient can be estimated with Eq. 10. Then the heat source function at the heat-affected layer is:

$$\dot{q} = \frac{Q}{V} \approx \frac{UA(T_a - T_b)}{\delta A} = \frac{UT_a}{\delta} \quad (11)$$

where Q is the heat flux from the outside wall to the ice slurry. V is the volume of the selected heat-affected layer close to the wall at the wash front. A is the annular outside surface area of the ice bed at the wash front. T_a is the ambient temperature. T_b is the wash front temperature, which is supposed to be zero degrees Celsius as suggested earlier. One can see at Eq. 11 that the value of the heat source function (\dot{q}) is greatly affected by the selected thickness (δ), highlighting the significance of the particle size of ice (and ripening time as well) in relation to channeling. The smaller the particle size, the thinner the heat-affected layer, and the greater the numerical value of the heat source function. The heat transfer coefficient (U) is also influenced by the thermal insulation outside the wash column. For acrylic (perspex) wall cylinder, four typical values of the heat source function are calculated using Eqs. 10, 11:

$\dot{q} = 0$ for the ideal adiabatic condition;

$\dot{q} = 2.0 \times 10^5 \text{ (Wm}^{-3}\text{)}$ for double-glazed jacket wall plus rubber foam insulation;

$\dot{q} = 5.64 \times 10^5 \text{ (Wm}^{-3}\text{)}$ for double-glazed jacket wall insulation;

$\dot{q} = 1.58 \times 10^6 \text{ (Wm}^{-3}\text{)}$ for single shell wall.

Table 4 shows more details of the impact of thermal insulation and thickness of the heat-affected layer on the values of U and \dot{q} . Using a typical values of the heat source function, $\dot{q} = 5.64 \times 10^5$, for the insulation of double-glazed jacket wall, another surfaces, S2, are generated in terms of Eq. 5, as shown in Figure 12a. The surface S1 represents the

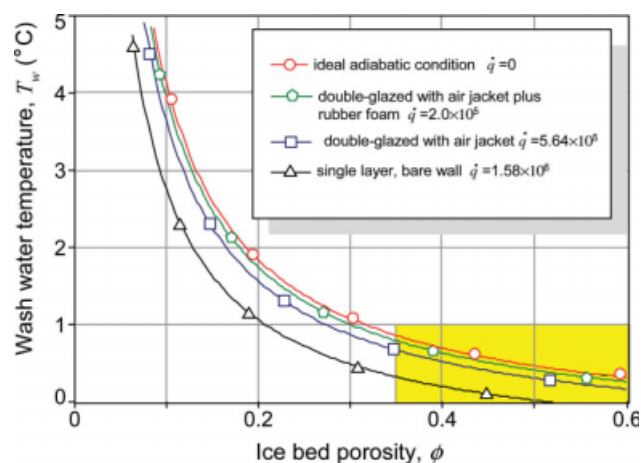


Figure 14. Model prediction of the criterion of wash front thawing which varies with the ice bed porosity in the heat-affected layer.

[Color figure can be viewed in the online issue, which is available at www.interscience.wiley.com.]

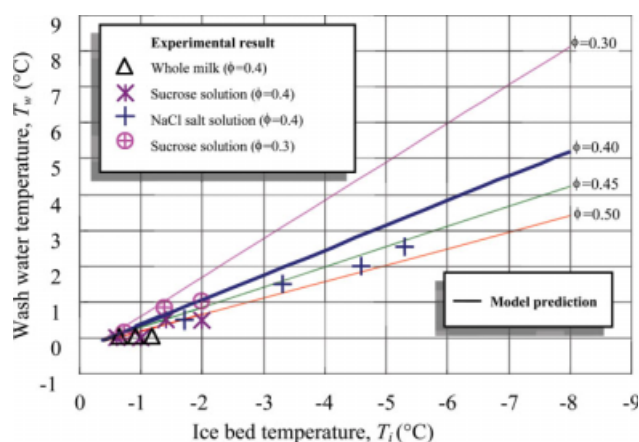


Figure 15. Criterion of wash front thawing (model predictions) and the experiment results of the wash water temperature under which good wash performance was obtained.

[Color figure can be viewed in the online issue, which is available at www.interscience.wiley.com.]

required wash water temperature inside the bulk ice bed but the surface S2 represents the required wash water temperature in the heat-affected zone close to the wall.

S2 is below S1 as shown in the 3D model implying that for the same bed porosity and bed temperature, the heat affected-layer requires a lower wash water temperature to counter-balance the heat input from environment to prevent ice thawing.

A typical scenario is that the ice bed temperature (T_i) is around -1 to -2°C ; and the heat-affected layer (δ) is 0.1 mm. To prevent ice thawing at the wash front in the vicinity of the wall, the first contact temperature (T) of wash water and ice (given by Eq. 4) should be $T \leq 0^\circ\text{C}$. Partial freezing of water will take place to sinter the washed ice bed. The relationship of $T_w - \phi - \dot{q}$ complies with Eq. 5. The chart of T_w versus ϕ is illustrated in Figure 14, where the values of \dot{q} highlighted in Table 4 are used for simulative calculation. The values of \dot{q} and U are obtained for different thermal insulations in terms of Eqs. 10, 11. It can be seen that the effect of the double-glazed jacket plus exterior rubber foam is very close to the ideal adiabatic condition. The values of ϕ from 0.3 to 0.6 are important because the porosity of a mechanically compressed ice bed falls into this region (as highlighted in Figure 14).

Model—experiment comparisons

As the piston pressure used for compressing the ice slurry was set to be 0.1 kg cm^{-2} in most experiments of this study,

the porosity of the obtained ice bed was accordingly 0.4 in terms of our previous calibration.⁸ In the 3D model shown in Figure 12, the model prediction of the wash water temperature that prevents ice thawing in the vicinity of the outside wall is given by the intersecting line of the surface S2 (green color) and the vertical semi-transparent yellow surface (at $\phi = 0.4$). The intersecting line itself is shown in blue color in Figure 12, and its projection on the $T_i - T_w$ plane is shown in Figure 15, in which the line ($\phi = 0.4$) keeps the same color.

Other projected lines in Figure 15 represent the model prediction of wash water temperature in different ice bed porosities.

Table 5 lists three groups of experiment data regarding the performance of the counter current wash column of ice bed. The ice beds were compressed from three types of ice slurry which was produced from FC of sucrose solutions, whole milk and NaCl salt solutions, respectively. In these trials, as mentioned earlier, the applied piston pressure was set 0.1 kg cm^{-2} or slightly higher, so the packed ice bed porosity was supposed to be 0.35 – 0.4 . Note the measured ice bed temperature T_i equaled the temperature of the mother liquid of the ice slurry. It was actually the equilibrium temperature, i.e., the freezing point, which was varying with the concentration C of the solutions. The model predictions of wash water temperature T_w were obtained in terms of Eq. 5, and the experimental wash water temperature T_{we} were measured when the satisfactory wash performance was observed. Let us take the experiment shown in Figure 9 as an example. The weight concentration of the NaCl salt solution was 6% , the ice bed temperature was -3.3°C , the model prediction of the wash water temperature was 1.94°C , and the observed satisfactory wash water temperature T_{we} was $\leq 1.5^\circ\text{C}$. These data composed the 11th column of Table 5. For each single solute concentration C in Table 5, there were actually at least three to four repetitive experimental points of wash water temperature T_{we} . The data presented in the table are the average values.

The model-experiment comparison of the wash water temperature is illustrated in Figure 15 by plotting the experimental data T_i and T_{we} listed in Table 5. Another group of test shown in Figure 15 (pink color) is the experiments in which the piston pressure was double (0.2 kg cm^{-2}), and the porosity of the ice bed was estimated to be 0.3 accordingly.

One can find that the experimental values are always below the model prediction in the chart. The maximum discrepancy between the model prediction and experiment is within 0.8°C . This may result from two reasons.

First, the model prediction is originally the criterion of wash front thawing, which is defined as the wash water temperature at which ice would neither growth nor thaw. But

Table 5. Model Prediction and Experimental Measurement of the Wash Water Temperature that Prevents Channeling in Packed Ice Beds with Porosity of 0.4

Sucrose Solution					Whole Milk				NaCl Salt Solution			
C	10	15	20	25	10	15	20	25	3	6	8	9
T_i	-0.6	-1.0	-1.4	-2.0	-0.4	-0.6	-0.9	-1.2	-1.7	-3.3	-4.6	-5.3
T_w	0.08	0.35	0.63	1.04	-0.06^*	0.11	0.29	0.49	0.84	1.94	2.80	3.31
T_{we}	0.0	0.0	0.5	0.5	$-^{**}$	0.0	0.0	0.0	0.5	1.5	2.0	2.5
Δ	0.08	0.15	0.13	0.54	—	0.11	0.29	0.49	0.34	0.44	0.80	0.81
$\bar{\Delta}$	0.39											

*The model prediction temperature is negative, this is not practical implying ice is still thawing even 0°C wash water is used.

**Channeling was observed even though 0°C wash water was used.

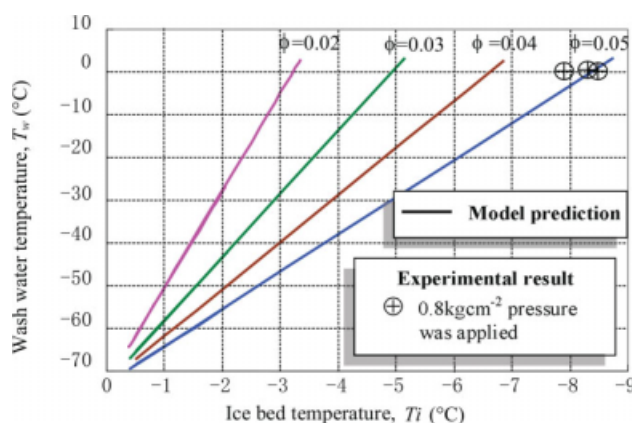


Figure 16. Criterion of wash front clogging (model predictions) and the experimental results of the wash water temperature under which wash front clogging occurred.

[Color figure can be viewed in the online issue, which is available at www.interscience.wiley.com.]

this temperature does not guarantee viscous fingering won't happen. However, the experimental results shown in Figure 15 represent the wash water temperature under which good wash performance was observed. Actually as discussed in the "Mobility Ratio," ice growth at the wash front is important to produce a mobility ratio $M < 1$ —a criterion that must be satisfied for a stable displacement without viscous fingering. That is to say, only by using colder wash water than the model prediction can we avoid the viscous fingering, and only by avoiding the viscous fingering can we obtain a well defined, horizontal wash front. In the experiment of washing a packed ice bed, sometimes it was hard to distinguish channeling from viscous fingering. So we could only record the "good wash" conditions.

Second, the discrepancy might partially ascribe to experimental errors involving the following aspects: (1) The porosity in the packed ice bed was varying slightly due to the dynamic compression process (model prediction assumes that it was 0.4); (2) The heat source function \dot{q} may be varying too in different experiments due to the change of ambient temperature, but the ambient temperature was assumed to be 20°C in model predictions; (3) The measurement error of the wash water, which was estimated to be $\pm 0.2^\circ\text{C}$ in this study; and (4) The observation error induced by the experiment operator. Among the four aspects mentioned earlier, the last one may be the most influencing, and it is unable to be quantified. Generally speaking, the model prediction is satisfactory in giving the suitable wash water temperature that prevents channeling in washing the packed ice bed.

The comparison of the criterion of wash front clogging (model prediction) and the experimental result was found even harder, for the wash water (usually tap water) could not be chilled to a required subfreezing temperature. Only three experiments with wash water close to 0°C gave reasonable results which were shown in Figure 16. In these experiments 40 kg compressing force was applied to form the ice bed (see Table 3). The bed porosity was estimated to be 0.05. A higher compressing force and a lower bed porosity could not be obtained in our current experiment apparatus.

Therefore, further experiments using thicker solutions with lower freezing points, so as to produce a lower ice bed temperature T_i , e.g., $< -10^\circ\text{C}$, instead of using more highly compressed ice beds should be done in the future to verify or modify the model of wash front clogging.

Conclusion

Thawing and freezing may both occur during the washing of ice beds in various locations. The former leads to channeling. The latter joins the adjacent ice particles, which helps to stop channeling and viscous fingering. However, over growth of ice may produce dead-end pores and cause liquid entrainment in the washed ice bed. The movement of the wash front tends to induce viscous fingering during the wash of the ice bed, while gravity is a stabilizing factor that keeps the wash front horizontal. Experimental study also showed how the wall effect of packed bed and the ambient temperature impact the wash performance.

Thermal analysis of this study revealed three criterions in achieving a horizontal, sharp and well-defined wash front.

1. The wash water temperature must be less than or equal to the value of criterion of wash front thawing to prevent channeling.

2. The mobility ratio at the wash front must be < 1 to prevent viscous fingering. Because of this, the wash water temperature must be even lower than the value of the criterion of wash front thawing to allow ice growing at the wash front.

3. The wash water temperature must be greater than the value of the criterion of wash front clogging due to over crystallization of ice. This allows wash water to pass through the ice bed and displace the mother liquid.

The mathematic model established in this study can be illustrated as a 3D image, which visually relates the operating variables, such as the wash water temperature, ice bed temperature, ice bed porosity, etc with the thermal behaviors, such as freezing and thawing, of the ice bed. The model explains the experimental results and gives a new insight into the operation of the packed ice wash column.

Acknowledgment

The authors thank Dr. Sashini Premathilaka for helping in completing this article. The authors acknowledge the partial sponsorship of the Chinese National Nature Science Foundation to this research.

Notation

- A = the annular outside surface area of the ice bed at the wash front, m^2
- b_1, b_2, b_3, b_4 = thickness of the inside wall, air jacket, outside wall, and rubber foam, respectively, m
- B_{wi} = ratio of volumetric thermal capacity of water and ice ($B_{wi} = \frac{\rho_w c_w}{\rho_i c_i} \approx 2.18$)
- B_f = volumetric ratio of liquid and ice in the ice bed ($B_f = \frac{\phi}{1-\phi}$)
- c_i = thermal capacity of ice ($=2100$), J kg^{-1}
- c_w = thermal capacity of water ($=4200$), J kg^{-1}
- C = solute concentration in weight percentage (kg solute/100 kg solution), %
- D_p = diameter of the individual ice particle, m
- h_{air} = natural convective individual heat transfer coefficient, $\text{W m}^{-2} \text{ } ^\circ\text{C}^{-1}$
- K_w = permeability of water in washed ice bed, m^2
- K_l = permeability of the mother liquid in unwashed ice bed, m^2

M = mobility ratio,
 \dot{q} = heat source function, W m^{-3}
 Q = heat flux input at the wash front from environment to the wash column ($Q = UAT_a$), W
 T = first contact temperature between water and ice, $^{\circ}\text{C}$
 T_a = ambient temperature, $^{\circ}\text{C}$
 T_b = wash front temperature ($=0$), $^{\circ}\text{C}$
 T_i = ice bed temperature, $^{\circ}\text{C}$
 T_w = wash water temperature below which ice thawing can be avoided (model prediction), $^{\circ}\text{C}$
 T_{we} = wash water temperature that results in satisfactory wash front (experiment), $^{\circ}\text{C}$
 v = interstitial velocity of the mobile phase in the ice bed, m s^{-1}
 δ = thickness of the heat-affected zone in the vicinity of the wall in the ice bed, M
 Δ = discrepancy of the model prediction and the experimental measurement of the wash water temperature ($\Delta = T_w - T_{we}$), $^{\circ}\text{C}$
 ΔH = freezing heat of water ($=334,000$), J kg^{-1}
 ϕ = original porosity of the unwashed ice bed
 ϕ_f = final porosity of the washed ice bed
 η_l = viscosity of the mother liquid, Pa s
 η_w = viscosity of the wash water, Pa s
 λ_l = thermal conductivity of the mother liquid, $\text{W m}^{-1} ^{\circ}\text{C}^{-1}$
 $\lambda_1, \lambda_2, \lambda_3, \lambda_4$ = thermal conductivity of the inside wall, air, outside wall, and rubber foam, respectively, $\text{W m}^{-1} ^{\circ}\text{C}^{-1}$
 ρ_i = density of ice ($=917$), kg m^{-3}
 ρ_l = density of the mother liquid, kg m^{-3}
 ρ_w = density of wash water ($=1000$), kg m^{-3}

Literature Cited

- McCabe WL, Smith JC, Harriott P. *Unit Operations of Chemical Engineering*, 6th ed. Boston: McGraw-Hill, Inc., 2001:1114.
- Geankoplis CJ. *Transport Processes and Unit Operations*, 2nd ed. Boston: Allyn and Bacon, Inc., 1983.
- Smith CE, Schwartzberg HG. Ice crystal size changes during ripening in freeze concentration. *Biotechnol Process*. 1985;1:111–120.
- Thijssen H. Freeze concentration. In: Spicer A, editor. *Advances in Preconcentration and Dehydration of Foods*. Wiley, 1974:115–149.
- Haq EU. Freeze purification of water utilizing a cold plastic surface and ice-liquid separation with a centrifuge. *Sep Sci Technol*. 1996;31:1971–1977.
- Muller JG. Freeze concentration of food liquids: theory, practice and economics. *Food Technol*. 1967;21:49–61.
- Huige NJJ, Thijssen HAC. Production of large crystals by continuous ripening in a stirrer tank. *J Cryst Growth*. 1972;13/14:483–487.
- Qin FGF, Chen XD, Premathilaka S, Free KW. Experimental study of wash columns used for separating ice from ice-slurry. *Desalination*. 2008;218:223–228.
- Jansens PJ, van der Ham R, Bruinsma OSL, van Rosmalen GM, Matsuoka M. The purification process in hydraulic wash column. *Chem Eng Sci*. 1995;50:2717–2729.
- van Oord-Knol L, Bruinsma OSL, Jansens PJ. Dynamic behavior of hydraulic wash columns. *AIChE J*. 2002;48:1665–1678.
- Jansens PJ, Bruinsma OSL, van Rosmalen GM. Compressive stresses and transport forces in hydraulic packed bed wash columns. *Chem Eng Sci*. 1994;49:3535–3543.
- van der Gun MA, Bruinsma OSL, van Rosmalen GM. Pastille purification in a gravity wash column. *Chem Eng Sci*. 2001;56:2381–2388.
- Verdoes D, Arkenbout GJ, Buirnsma OSL, Koutsoukos PG, Ulrich J. Improved procedures for separating crystals from the melts. *Appl Therm Eng*. 1997;17:789–888.
- Thomsen K, Rasmussen P, Gami R. Simulation and optimization of fractional crystallization processes. *Chem Eng Sci*. 1994;53:1551–1564.
- Qin FGF, Chen XD, Ramachandra S, Free K. Heat transfer and power consumption in a scraped-surface heat exchanger while freezing aqueous solutions. *Sep Purif Technol*. 2006;48:150–158.
- Qin FGF, Premathilaka S, Chen XD, Free KW. The shaft torque in a laboratory scraped surface heat exchanger used for making ice slurries. *Asia-Pacific J Chem Eng*. 2007;2:618–630.
- Qin FGF, Chen XD, Russell AB. Heat transfer at the subcooled-scraped surface with/without phase change. *AIChE J*. 2003;49:1947–1955.
- Qin FGF, Chen XD, Farid MM. Growth kinetics of ice films spreading on a subcooled solid surface. *Sep Purif Technol*. 2004;39:109–121.
- Mersmann A, editor. *Crystallization Technology Handbook*. New York, Basel, Hong Kong: Marcel Dekker, Inc, 1995:314,316.
- Mullin JW. *Crystallization*, 4th ed. Oxford, etc.: Butterworth-Heinemann, 2001.
- Pronk P, Infante Ferreira CA, Witkamp GJ. A dynamic model of Ostwald ripening in ice suspensions. *J Cryst Growth*. 2005;275: e1355–e1361.
- Pronk P, Hansen TM, Infante Ferreira CA, Witkamp GJ. Time-dependent behavior of different ice slurries during storage. *Int J Refrig*. 2005;28:27–36.
- Thijssen HAC. Apparatus for the separation and treatment of solid particles from a liquid suspension. U.S. Pat. 3,872,009, 3,872,009, 1975.
- Thijssen HAC. Continuous packed bed wash column. U.S. Pat. 4,475,355, 4,475,355, 1984.
- den Dass J, Grenco. Current large-scale commercial application of freeze concentration in the food industry. *Eur Food Drink Rev*. 1991;Spring:19–24.
- Williamson A-M, Lips A, Clark A, Hall D. Ripening of faceted ice crystals. *Powder Technol*. 2001;121:74–80.
- Sahimi M. *Flow and Transport in Porous Media and Fractured Rock: From Classical Methods to Modern Approaches*. Weinheim: VCH Verlagsgesellschaft MbH, 1995.
- Choy B, Reible DD. *Diffusion Models of Environmental Transport*. Boca Raton: Lewis Publishers, 1999.
- Greenkorn RA. *Flow Phenomena in Porous Media: Fundamentals and Applications in Petroleum, Water, and Food Production*. Marcel Dekker, Inc., 1983.
- Kang C, Yano S, Okada M. Non-uniform melting in packed beds of fine ice slurry. *Int J Refrig*. 2001;24:338–347.

Manuscript received Oct. 26, 2007, revision received Jan. 31, 2009, and final revision received Mar. 16, 2009.